

Jason P. Evans* and Ronald B. Smith
Yale University, New Haven, Connecticut, U.S.A.

1. INTRODUCTION

The *Fertile Crescent* is defined here as an area encompassing south-east Turkey, north-eastern Syria, northern Iraq and north-western Iran and is shown in Figure 1. The area includes most of the headwaters of the Tigris River and hence precipitation here is an important source of fresh water for parts of Turkey and Iraq. Being a dominantly arid area relatively little precipitation recycling occurs over the land and the surrounding water bodies are major contributors to atmospheric water vapor. To the northwest is the Black Sea, northeast is the Caspian Sea, to the west is the Mediterranean and to the south is the Persian Gulf. While it has been generally accepted that the area is dominated by storm systems which move in from the Mediterranean Sea, earlier modeling work (Evans, J.P. et al., 2004) indicated that water vapor contributing to some of these storm events is dominated by a southerly flux. Quantifying the significance of this contribution provides some indication of Fertile Crescent precipitation sensitivity to changes in the condition of the Persian Gulf relative to the Mediterranean Sea. This may have important implications for human settlement during the Holocene when the Persian Gulf is known to have changed substantially (Aqrabi, A. A. M., 2001; Lambeck, K., 1996).

GCM simulations of the mid-Holocene climate also indicate that the African Monsoon was further north than at present Braconnot, P. et al. (2000) possibly having significant impact on the Saudi Peninsula. If this was the case then a significantly larger body of water vapor would have been present in the southern Middle East region derived largely from the waters of the Red Sea, Arabian Sea and Persian Gulf. Given significant isotopic differences between these bodies of water and others nearby (Mediterranean, Black and Caspian Seas) it may be possible use isotopic analysis of paleo-records to determine what influence these

monsoon related changes in the southern portion of the domain had on the Precipitation in the Fertile Crescent. A first step towards this is understanding what role is played by water vapor fluxes from the South today and what conditions may have led to significant changes in the past.

Creating a synoptic climatology for the region identifies persistent atmospheric regimes and their distribution through time. In this study an Empirical Orthogonal Function (EOF) based map-pattern classification is performed along with a classification based more directly on water vapor fluxes through the region. Observations of atmospheric water vapor at high temporal and spatial resolution do not currently exist hence a high resolution Regional Climate Model (RCM) simulation was used to investigate the water vapor fluxes (section 2). Synoptic climatologies are established using both the EOF map-pattern classification approach and a more direct clustering according to the water vapor fluxes into and out of the region (section 3) with the results and conclusions of the study presented in sections 4 and 5 respectively.

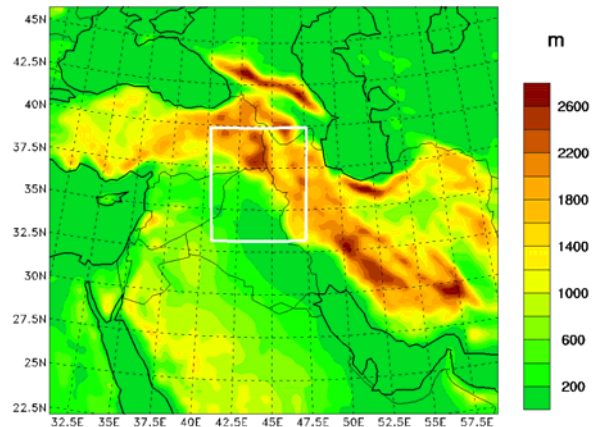


Figure 1: Topography of regional climate model domain (*Fertile Crescent* study area is outlined in white).

* Corresponding Author address: Jason P. Evans, Yale University, Dept. of Geology and Geophysics, New Haven, CT, USA, 06520. email: Jason.evans@yale.edu

2. REGIONAL CLIMATE MODEL (MM5-NOAH)

The PSU/NCAR (Pennsylvania State University / National Center for Atmospheric Research) mesoscale modeling system MM5 is described in Dudhia (1993) and Grell, G. A. et al. (1994). MM5 is a limited-area nonhydrostatic model that uses a terrain-following vertical coordinate system. It has 2-way nesting capabilities, and flexible physics options. In this study MM5 was implemented with the Reisner Mixed-Phase explicit moisture scheme (Reisner, J. et al., 1998), the MRF planetary boundary layer scheme (Hong, S. Y. and Pan, H. L., 1996), the Rapid Radiative Transfer Model (RRTM) radiation scheme (Mlawer, E. J. et al., 1997) and the Grell scheme for convective precipitation (Grell, G. A. et al., 1994).

MM5 is operationally linked with the NOAH LSM. NOAH is a direct descendent of the Oregon State University (OSU) LSM (Mahrt, L. and Ek, M., 1984; Mahrt, L. and Pan, H. L., 1984; Pan, H. L. and Mahrt, L., 1987), a sophisticated land surface model that has been extensively validated in both coupled and uncoupled studies (Chen, F. and Mitchell, K., 1999; Chen, F. and Dudhia, J., 2001). The NOAH LSM simulates soil moisture, soil temperature, skin temperature, snowpack depth and water equivalent, canopy water content, and the energy flux and water flux terms of the surface energy balance and surface water balance. In its MM5-coupled form NOAH has a diurnally dependent Penman potential evaporation (Mahrt, L. and Ek, M., 1984), a four layer soil model (Mahrt, L. and Pan, H. L., 1984), a primitive canopy model (Pan, H. L. and Mahrt, L., 1987), modestly complex canopy resistance (Jacquemin, B. and Noilhan, J., 1990), and a surface runoff scheme (Schaake, J. C. et al., 1996).

MM5 has been applied successfully at grid cell resolutions ranging from greater than 100 km to less than 1 km and is used for both weather forecasts and climate research. Here we apply the model at 25km horizontal resolution over a domain which includes much of the Middle East and the surrounding water bodies. Figure 1 shows the model domain excluding the rows and columns which are directly influenced by the boundary conditions. This domain was initialized for a simulation beginning in November 1989 with initial and boundary conditions obtained from the NCEP/NCAR reanalysis. The first two months of model run are discarded, allowing fields such as soil moisture to "spin-up", and the following five years (1990 thru 1994) are simulated. The model was run with 23 vertical levels which were spaced more tightly near the ground surface.

Previously an identical simulation was performed with the RegCM2 regional climate model which was extensively evaluated against multiple datasets (Evans, J.P. et al., 2004). This MM5 simulation was evaluated against the same datasets and found to be an improvement over the RegCM2 simulation in a number of ways. The MM5 run significantly reduces the wintertime cold bias and seasonal temperature errors present in the RegCM2 run. The precipitation fields are also improved with the MM5 run having generally smaller bias and much improved pattern correlation compared to the observations.

3. SYNOPTIC CLIMATOLOGY

A synoptic climatology was created by applying an EOF-based map-pattern classification to maps of the daily 500hPa geopotential height using the procedure given in Yarnal (1993). The number of EOFs to use is established by examination of a Scree plot and varimax rotation is applied to the EOF component loadings. Days are then clustered using the ISODATA clustering algorithm where the number of classes is chosen using the R^2 metric discussed in Kalkstein, L. S. et al., 1987. These classes are then compared to precipitation and water vapor fluxes through the Fertile Crescent area shown in Figure 1.

Given the high spatial and temporal resolution of data available from the RCM a classification based on the fluxes through the sides of the box shown in Figure 1 is also created. Each event is represented by a data series consisting of a three hourly flux series from each direction (North, South, East, and West) and the precipitation series. These series extend from one day before, until one day after the time of peak precipitation. The use of all the major fluxes guarantees that the complete data series has a mean close to zero regardless of the size of event and removes the potential for the clustering algorithm to cluster points based on differences in their means.

This clustering is performed using the iterative clustering algorithm ISODATA applied to the above data series for the 200 largest precipitation events over the five year period. These events produce a minimum of ~0.84mm of precipitation over two days. In total they account for ~68% of all the precipitation falling within the box indicated in Figure 1 over the five year period.

The algorithm was run using statistical initialization starting with five, seven and ten classes. In all cases only five classes of events were produced by the algorithm. That is, when starting with more than five classes the algorithm found it necessary to merge classes due to their

similarity until only five classes remained. This increases the confidence that this five class clustering is a robust result. This classification is here-after referred to as the WV-based climatology.

4. RESULTS

EOF based synoptic climatology results in 14 classes. The mean 500hPa geopotential height for each of these classes is shown in Figure 3. The monthly distribution is shown in Figure 2. Summertime conditions are predominantly classes 8, 9 and 10. Class 7 is most common during the transition seasons. The remaining 11 classes account for most of the precipitation events which occur during winter. Closer inspection of the EOF-based classes reveals no significant relationship with Fertile Crescent precipitation or with the water vapor fluxes.

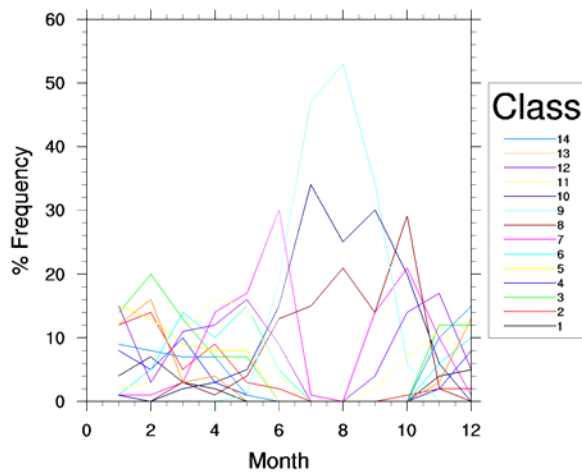


Figure 2: Percent Frequency distribution of EOF-based synoptic climatology classes by Month

Figure 4 presents the 500hPa geopotential heights of the water vapor flux based. Comparison of Figure 3 with Figure 4 reveals a number of similarities. Class 1 of the WV-based climatology is similar to class 2 of the EOF-based climatology. Class 2 of the WV-based resembles class 3 of the EOF-based climatology although the EOF-based class has a significantly deeper low. Class 4 of the WV-based classification resembles class 6 of the EOF-based system. Classes 3 and 5 of the WV-based climatology do not obviously have an analogue in the EOF-based climatology.

The mean water vapor fluxes for each of the classes produced by the WV-based classification are presented in Figure 5. In every case fluxes from the West and South tend to be into the box while fluxes from the East and North tend to be out of the box. The flux of water due to precipitation is considered to be out of the atmospheric box. Focusing on the incoming fluxes, the events are split according to the relative importance of westerly and southerly fluxes. Classes 1 and 2 are dominated by westerly fluxes, while classes 4 and 5 are dominated by southerly classes. Class 3 has a dominant southerly flux just before reaching the precipitation peak, this flux then rapidly decreases and the system is again dominated by the westerly flux.

Events in class 1 tend to produce the least amount of precipitation overall. The magnitude of all the fluxes tends to increase with increasing class number, with events in class 5 producing the most precipitation. In fact class 5 includes 3 out of the 4 largest precipitation events. Excluding class 1, the peak in total incoming water flux occurs ~6 hours before the peak in precipitation.

Table 1: Number of events and % precipitation in each class

Class	Number of Events	% Total Precipitation
1	48 (24%)	9
2	64 (32%)	25
3	58 (29%)	30
4	26 (13%)	28
5	4 (2%)	8

Several quantitative conclusions can be drawn from the number and size of events in each class as presented in Table 1. The majority of events are dominated by westerly fluxes (56%) in accordance with widespread belief. These events however account for 34% of the total precipitation. Extending this to include events in which the westerly flux significantly contributes accounts for 85% of precipitation events and 64% of the total precipitation. Only 15% of the events are dominated by southerly fluxes, however these events tend to be large and account for ~36% of the total precipitation.

This implies that storm systems which produce large southerly fluxes of water vapor, while relatively rare, are very important in the cumulative precipitation total. The presence or absence of a

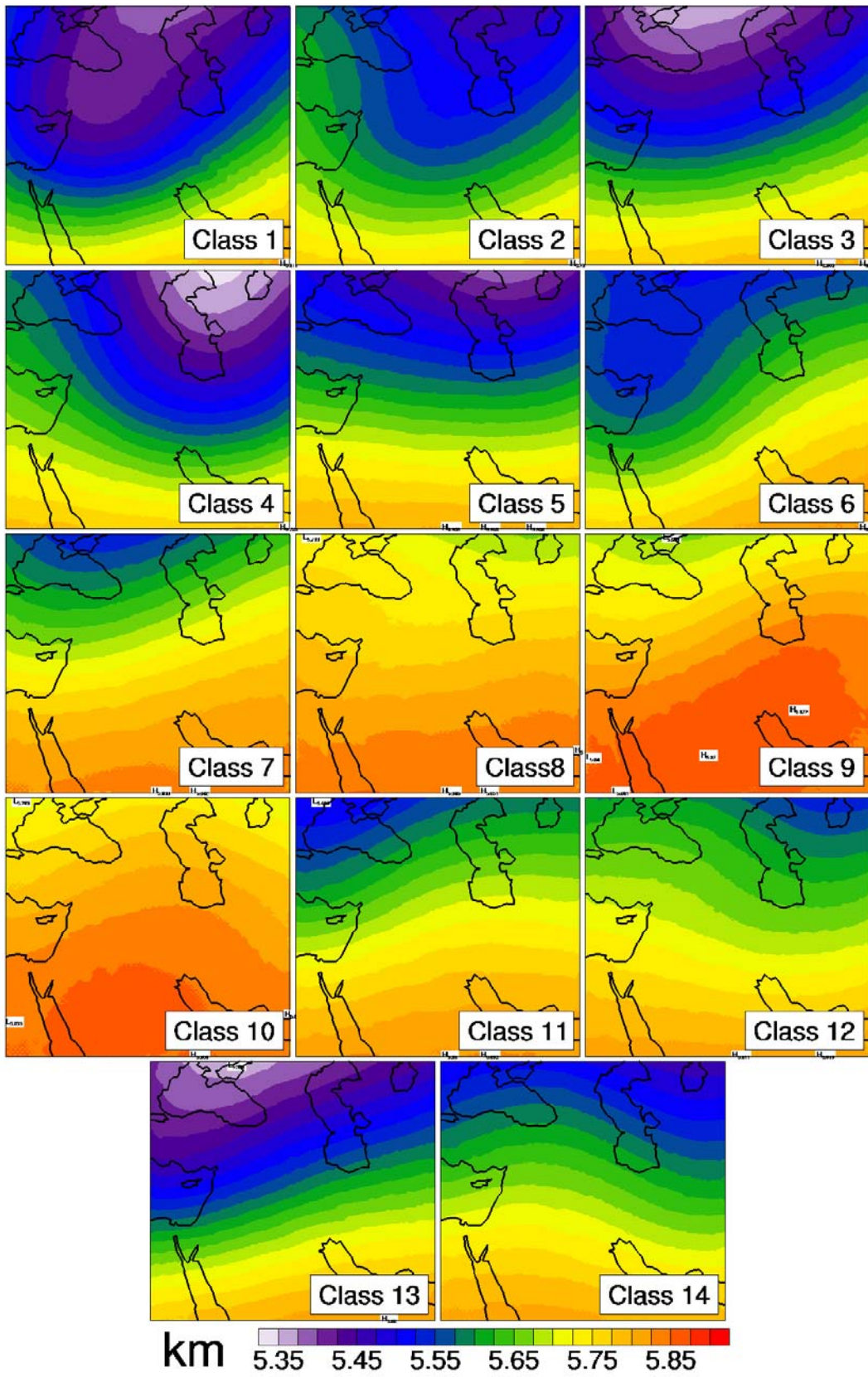


Figure 3: 500hPa geopotential heights for EOF-based synoptic climatology.

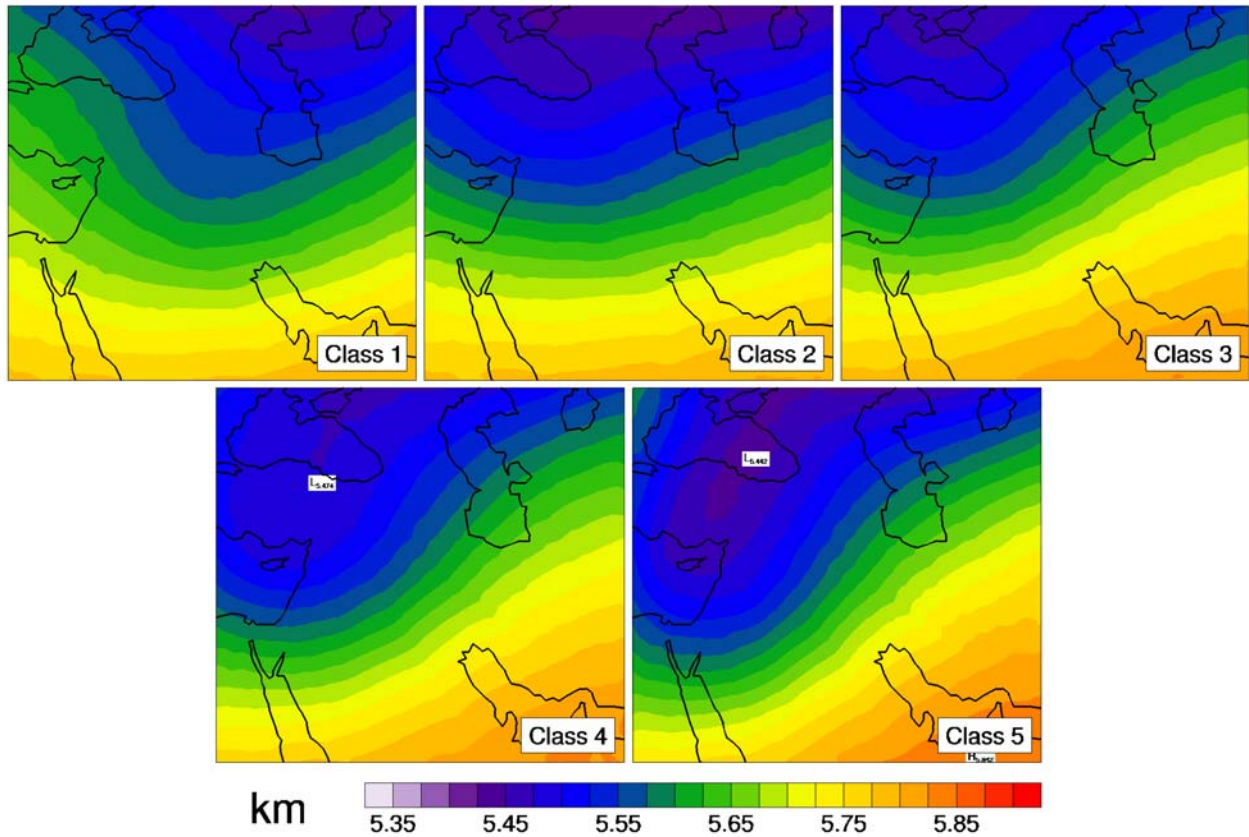


Figure 4: 500hPa geopotential heights for each WV- based class.

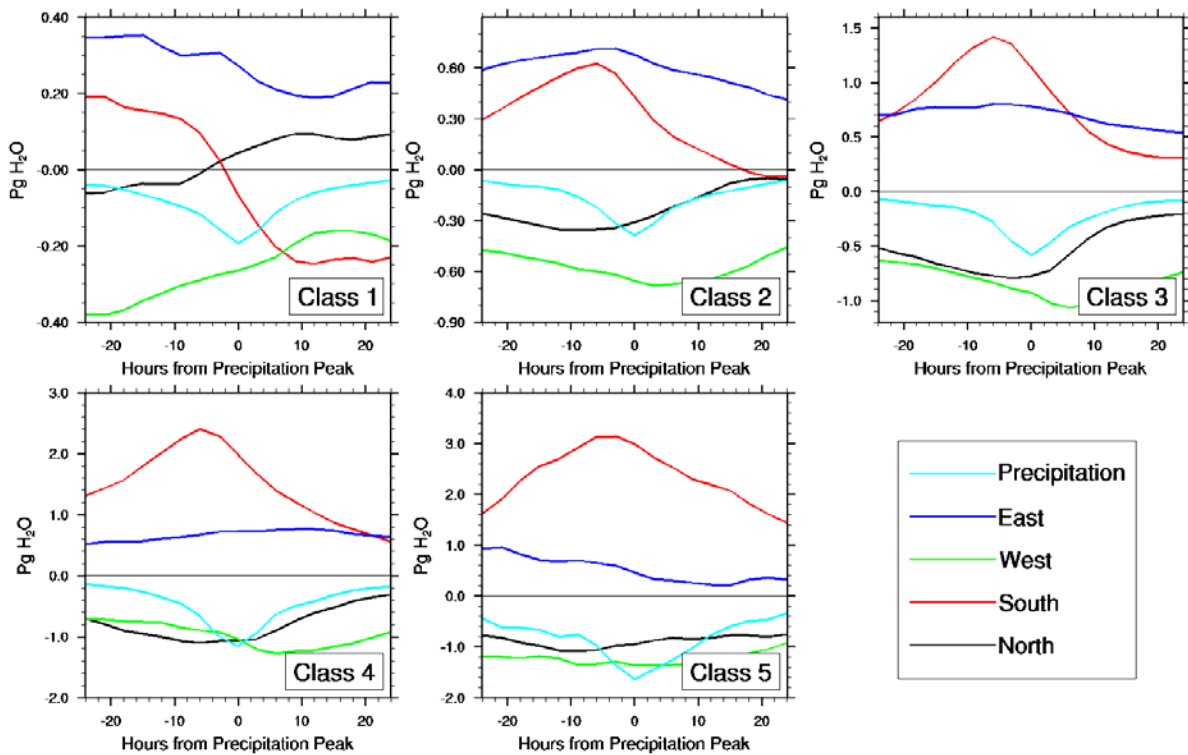


Figure 5: Water vapor flux into the Fertile Crescent for each WV-based class.
 Note on the legend: East is GREEN and West is BLUE.

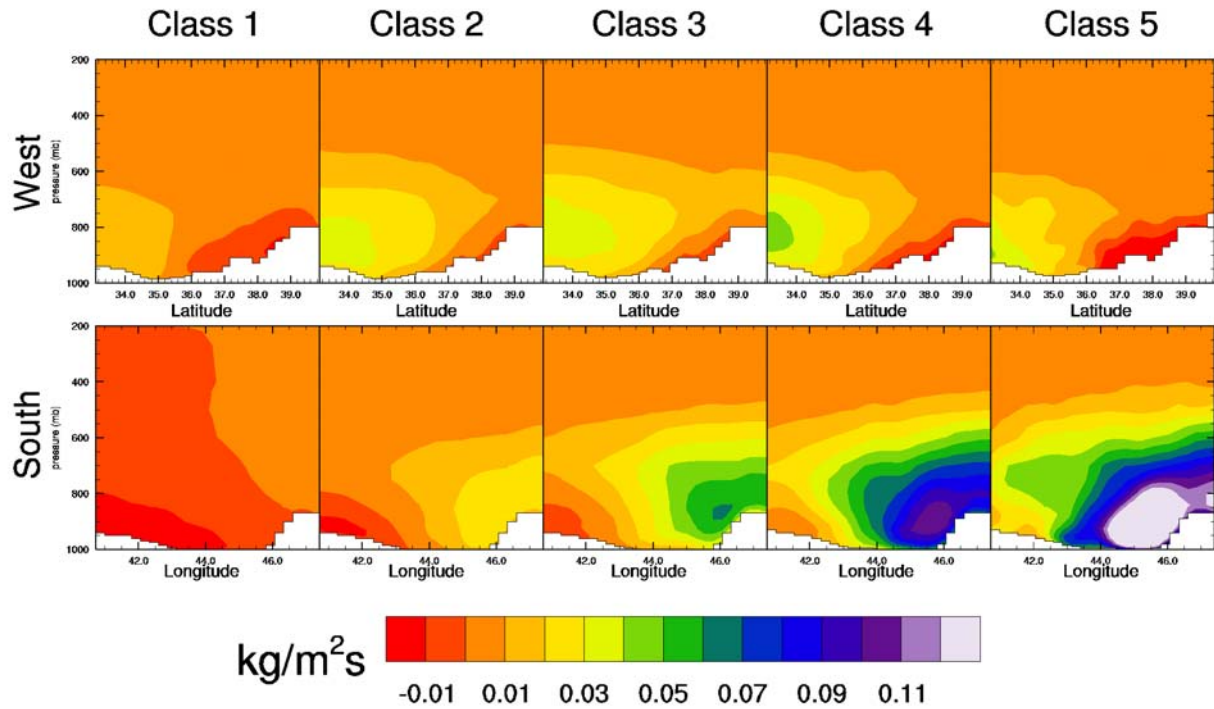


Figure 6: Vertical cross sections of the water vapor flux crossing the West and South sides of the Fertile Crescent box, 3 hours before the precipitation peak (topography is outlined and shown in white).

few of these events may be the difference between an average and a poor precipitation year.

Using an RCM also provides detail in the vertical direction allowing the vertical distribution of water vapor fluxes to be investigated. Figure 6 shows the water vapor flux into the box shown in Figure 1, from the West and from the South, for each class. Class 1 appears significantly different from the other classes with the South flux being principally out of the box and the West flux being confined to the southernmost 2/3 of the domain. The influx from the West is more intense and widespread in every other class, extending across the entire domain for class 3. Class 5 is unique in having a significant West outflux which is confined to the mountainsides of Northern Syria/Southern Turkey. The influx from the South becomes progressively more intense with each class, with the maximum influx above the slopes of the Zagros Mountains. While most of the southerly flux is above the Euphrates-Tigris valley, classes 3, 4 and 5 show increasing evidence of the flux spilling over the Zagros Mountains to the East.

5. CONCLUSIONS

The study presented here attempts to quantify the significance of southerly water vapor fluxes on precipitation occurring in the Fertile Crescent region. The possibility of this was suggested by previous modeling work and confirmed through investigation of the NVAP dataset that combines data from several observational platforms (not shown). The water vapor fluxes were investigated at high temporal and spatial resolution by using a Regional Climate Model (MM5-NOAH) to downscale the NCEP/NCAR reanalysis. An EOF-based synoptic climatology based on the 500hPa geopotential height was created but the classes were found to only poorly differentiate between water vapor flux states. These fluxes were addressed directly using the ISODATA clustering algorithm on the 200 largest precipitation events occurring during the first 5 years of the 1990s and accounting for over 2/3 of the entire precipitation, in order to group these events into classes based on the similarity of their water vapor fluxes.

Results indicate that while southerly fluxes were significant in 44% of precipitation events, these events account for 66% of the precipitation.

In fact southerly fluxes were dominant in 15% of events but these events produced 36% of the total precipitation. Thus, while the vast majority of precipitation events occurring in the Fertile Crescent originated as water vapor advected from the West, those events which included southerly fluxes produced much larger precipitation totals. This suggests that changes which may affect these southerly fluxes more than the westerly fluxes (e.g. changes in the Indian monsoon, movement of the Persian Gulf, etc.) may have a relatively strong affect on the total precipitation falling in the Fertile Crescent even though they affect relatively few precipitation events.

6. ACKNOWLEDGEMENTS

This study was undertaken with the financial support of NASA (EOS/03-0587-0425) and NSF (ATM-0112354). We appreciate computer time for model runs provided by National Center for Atmospheric Research (NCAR). The research was motivated and assisted by many fruitful conversations with other members of the South-West Asia project team including Roland Geerken, Frank Hole, Ben Zaitchik, Eddy De Pauw and Larry Bonneau.

7. REFERENCES

- Aqrabi, A. A. M., 2001: Stratigraphic signatures of climatic change during the Holocene evolution of the Tigris-Euphrates delta, lower Mesopotamia. *Global and Planetary Change*, **28**, 267-283.
- Braconnot, P., S. Joussaume, N. de Noblet, and G. Ramstein, 2000: Mid-holocene and Last Glacial Maximum African monsoon changes as simulated within the Paleoclimate Modelling Intercomparison Project. *Global and Planetary Change*, **26**, 51-66.
- Chen, F. and K. Mitchell, 1999: Using GEWEX/ISLSCP forcing data to simulate global soil moisture fields and hydrological cycle for 1987-1988. *Journal of the Meteorological Society of Japan*, 1-16.
- Chen, F. and J. Dudhia, 2001: Coupling an advanced land surface-hydrology model with the Penn State-NCAR MM5 Modeling system. Part II: Preliminary model validation. *Monthly Weather Review*, 587-604.
- Dudhia, J., 1993: A nonhydrostatic version of the Penn-State/NCAR mesoscale model: Validation tests and simulation of an Atlantic cyclone and cold front
- Evans, J.P., R.B. Smith, and R.J. Oglesby, 2004: Middle East climate simulation and dominant precipitation processes. *International Journal of Climatology*, In Press.
- Grell, G. A., J. Dudhia, and D. R. Stauffer, 1994: A description of the fifth-generation Penn State/NCAR mesoscale model (MM5). *NCAR Tech. Note*, National Center for Atmospheric Research, 117.
- Hong, S. Y. and H. L. Pan, 1996: Nonlocal boundary layer vertical diffusion in a medium-range forecast model. *Monthly Weather Review*, 2322-2339.
- Jacquemin, B. and J. Noilhan, 1990: Sensitivity study and validation of a land surface parameterization using the HAPEX-MOBILHY data set. *Boundary Layer Meteorology*, 93-134.
- Kalkstein, L. S., G. R. Tan, and J. A. Skindlov, 1987: An Evaluation of 3 Clustering Procedures for Use in Synoptic Climatological Classification. *Journal of Climate and Applied Meteorology*, **26**, 717-730.
- Lambeck, K., 1996: Shoreline reconstructions for the Persian Gulf since the last glacial maximum. *Earth and Planetary Science Letters*, **142**, 43-57.
- Mahrt, L. and M. Ek, 1984: The influence of atmospheric stability on potential evaporation. *Journal of Climate and Applied Meteorology*, 222-234.
- Mahrt, L. and H. L. Pan, 1984: A two-layer model of soil hydrology. *Boundary Layer Meteorology*, 1-20.
- Mlawer, E. J., S. J. Taubman, P. D. Brown, M. J. Iacono, and S. A. Clough, 1997: Radiative transfer for inhomogeneous atmosphere: RRTM, a validated correlated-k model for the longwave. *Journal of Geophysical Research*, 16663-16682.
- Pan, H. L. and L. Mahrt, 1987: Interaction between soil hydrology and boundary-layer development. *Boundary Layer Meteorology*, 185-202.
- Reisner, J., R. J. Rasmussen, and R. T. Bruintjes, 1998: Explicit forecasting of supercooled liquid water in winter storms using the MM5 mesoscale model. *Quarterly Journal of the Royal Meteorological Society*, 1071-1107.
- Schaafe, J. C., V. I. Koren, Q. Y. Duan, K. Mitchell, and F. Chen, 1996: A simple water balance model (SWB) for estimating runoff at different spatial and temporal scales. *Journal of Geophysical Research*, 7461-7475.
- Yarnal, B., 1993: *Synoptic climatology in Environmental Analysis*. Belhaven Press, 195 pp.